Effects of Solidity, Number of Blades, and Chord Distribution on Rotor Performance in a Martian Environment

Gianmarco Sahragard-Monfared
Aerospace Engineer
NASA Ames Research Center
Moffett Field, CA

Joshua Bowman
Aerospace Engineer
Science and Technology Corp.
Moffett Field, CA

Witold J. F. Koning
Aerospace Engineer
Science and Technology Corp.
Moffett Field, CA

Wayne Johnson
Aerospace Engineer
NASA Ames Research Center
Moffett Field, CA

ABSTRACT

Rotor performance in a Martian environment was analyzed with an objective of increasing thrust with minimal impact on efficiency. The Sample Recovery Helicopter (SRH) and Rotorcraft Optimization for the Advancement of Mars Exploration (ROAMX) rotors were studied by varying solidity, blade count, and chord distribution to determine which configuration delivered the most desirable performance. For all configurations, the ROAMX rotor displayed better performance than the SRH rotor. It was observed that increasing solidity reduced the blade loading required to achieve the peak figure of merit, and beyond a solidity ratio of 0.3 the figure of merit was negatively impacted. For both rotors a 6-bladed configuration with a solidity ratio of 0.3 delivered the optimal figure of merit.

INTRODUCTION

The success of Ingenuity in not only serving as a technology demonstration but continuing for 72 research flights and assisting in the operation of Perseverance, has prompted further efforts in the development of Martian rotorcraft [Ref. 1]. To include further functionality in Martian rotorcraft, payload, and therefore required thrust, must both significantly increase. To improve rotorcraft performance, both new blade designs and rotorcraft configurations have been explored, discussed briefly as follows. Efforts such as Rotorcraft Optimization for the Advancement of Mars Exploration (ROAMX) have found that sharp edged, thin airfoils can provide significantly improved performance, while new rotorcraft configurations, such as the proposed Mars Science Helicopter (MSH) hexacopter, can provide greater thrust with increased rotor disc area [Refs. 2-5]. While rotorcraft in Earth's atmosphere are typically limited to a solidity ratio of 0.10 or lower, it may be advantageous to explore higher solidity rotors operating in the thinner Martian atmosphere. While power usage increases with higher solidity, higher solidity rotors have the benefit of a more compact footprint for generating higher thrust. Space conservation is of special concern for Martian rotorcraft, where the entire rotorcraft must be stored in the device used for entry, descent, and landing (EDL). This work focuses on the study of higher solidity rotors which might improve total thrust and efficiency, while still satisfying the EDL size constraints.

Presented at the Vertical Flight Society's 81st Annual Forum & Technology Display, Virginia Beach, VA, USA, May 20-22, 2025.

APPROACH

The rotors used for Ingenuity had a thrust-weighted solidity ratio of 0.148, using two blades for each rotor in a coaxial configuration. To maintain consistency, all solidities listed for the remainder of this work are thrust-weighted solidity. To fully explore the range of feasible rotor solidity ratios, it was desired to perform an analysis of potential rotors with solidity ratios as high as 0.50. Significant analysis for the Ingenuity rotor was completed using the Comprehensive Analytical Model of Rotorcraft Aerodynamics and Dynamics II (CAMRAD II) [Refs. 6 and 7]. Along with the analytical work performed for the Ingenuity rotor prior to its mission, CAMRAD II analysis was also used to model expected behavior from two test campaigns that used the Ingenuity rotor, Engineering Design Model I and the Transonic Rotor Test [Refs. 8 and 9]. For simpler comparison to the analysis of the Ingenuity rotor, CAMRAD II was also used for modeling the prospective rotors.

While Ingenuity serves as a model with both operational and experimental data, it was desired to study proposed blades that have been designed to improve rotor performance for Martian rotorcraft. The ROAMX blades have been manufactured and are being tested in hover at Martian pressure. The ROAMX blades are significantly different than the Ingenuity blade, both in airfoil and in chord and twist distributions. The ROAMX blade design and airfoil profiles as compared to Ingenuity are displayed in Figure 1. The ROAMX chord and twist distributions can be found in Ref. 1. The ROAMX rotor uses unconventional roamx-0201 and roamx-0202 parameterized airfoils to maximize performance in the compressible low-Reynolds number regime [Ref. 2]. The optimized ROAMX rotor is 6-bladed with a thrust-weighted solidity constrained to 0.25. However, due to experimental testing limitations, a 4-bladed ROAMX configuration with a thrust-weighted solidity of 0.167 was tested.

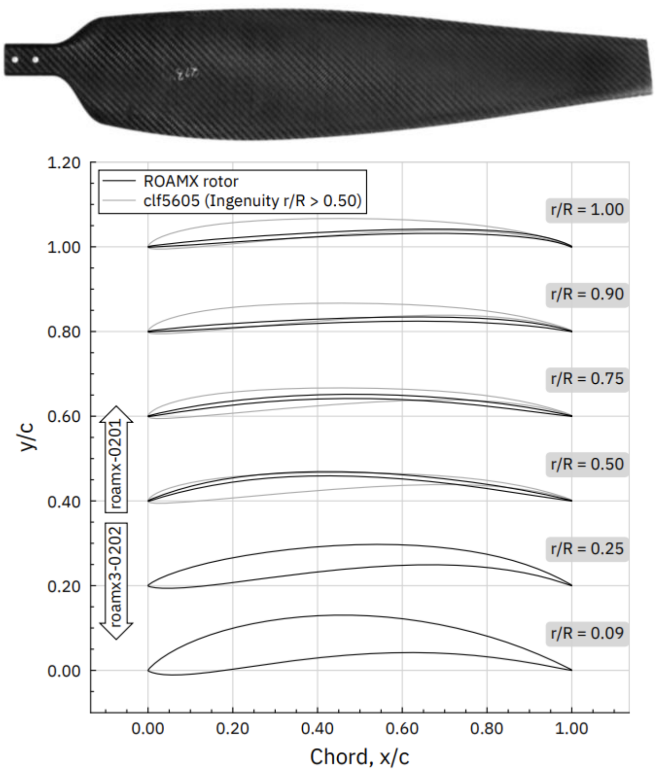

Figure 1. ROAMX blade design and airfoil profiles as compared to Ingenuity, from Ref. 2.

The same study on solidity effects was performed with the proposed blade form of the Sample Recovery Helicopter (SRH) [Refs. 2 and 10]. The SRH blade used the same airfoils as Ingenuity, but with a larger radius and slightly different chord and twist distributions to improve upon the performance of the Ingenuity rotor and allow for a higher payload. Prior to this study, extensive work had been completed on analysis of the Ingenuity blades and predictions of the planned SRH blades [Ref. 11]. The SRH blade design and airfoil profile is illustrated in Figure 2. The SRH chord and twist distributions can be found in Ref. 10. The standard solidity of the SRH 4-bladed configuration is 0.128. By observing the effects of solidity and blade number on two significantly different blades, both created for Martian operation, the effects should be evident.

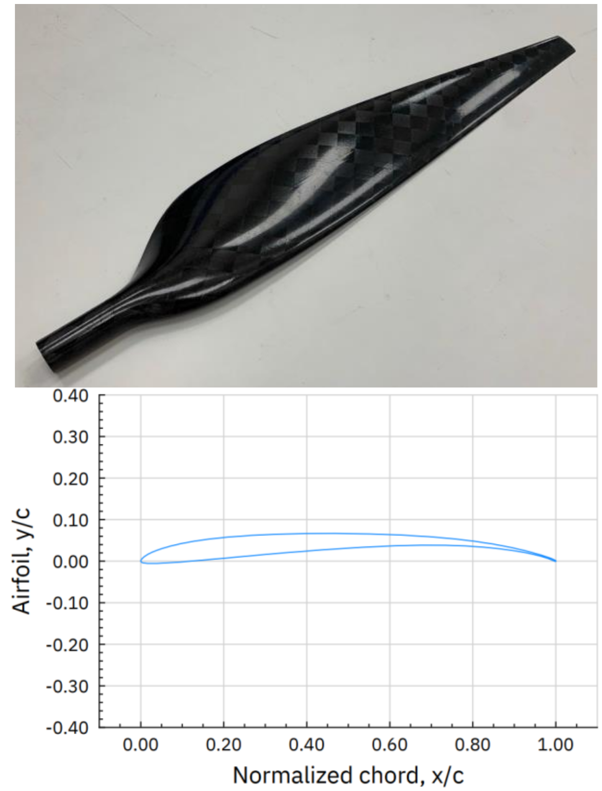

Figure 2. SRH prototype rotor blade (Credit: Langberg, S., AeroVironment, Inc.) and outboard airfoil profile, from Ref. 4.

To observe the effects of solidity ratios on rotor performance, a series of solidities were analyzed namely: 0.10, 0.15, 0.20, 0.25, 0.30, 0.35, 0.40, 0.45, and 0.50. In addition, the effects of different numbers of blades were also assessed, as blade shape could change significantly at high solidities depending on the number of blades. For each of the solidity ratios considered, 2-, 4-, 6-, and 8-bladed configurations were modeled. The full matrix of configurations assessed for both the ROAMX and SRH rotors is provided in Table 1.

Table 1. Modeled ROAMX and SRH Rotor Configurations.

Solidity Ratio	Number of Blades
0.10	2, 4
0.15	2, 4, 6
0.20	2, 4, 6, 8
0.25	2, 4, 6, 8
0.30	2, 4, 6, 8
0.35	2, 4, 6, 8
0.40	4, 6, 8
0.45	4, 6, 8
0.50	4, 6, 8

Computational inputs such as environmental and flight conditions were kept as similar as possible between both rotors despite a slight difference in densities at which each rotor's respective airfoil table was generated. Relevant CAMRAD II inputs are outlined in Table 2.

Table 2. CAMRAD II Inputs.

Rotor	Input	Value
ROAMX and SRH	Radius	0.64 m
ROAMX and SRH	M_{Tip}	0.78
ROAMX and SRH	Flight Condition	Hover
ROAMX and SRH	Collective	1-30°
ROAMX	Density	0.0170 kg/m^3
SRH		0.0156 kg/m^3

Solidity Scaling

To understand the effects of solidity and blade number only, the first analyses were performed using only chord-scaled versions of the SRH and ROAMX blades, using their respective airfoils. It is important to note that radius and twist values were kept constant throughout this study. These blade shapes at high solidity ratios often resulted in problematic geometries, with extremely large chords that result in overlap between the blades, as seen in Figure 3. Since CAMRAD II can operate even with blade overlap, this was not an issue directly. To accurately model rotor performance, the wake properties were modified within CAMRAD II to mitigate overlapping wakes at low collective values resulting in convergence issues or aberrant behavior. Specifically, special consideration needed to be given to vortex core growth in the wake to avoid convergence issues. A dedicated Viscous Vortex Particle Method rotor wake modeling study of these high solidity rotors in a Martian atmosphere can be found in Ref. 12. To still assess more realistic blades with these solidities, different coarse blade shape modifications were used to generate blades with matching solidity while avoiding overlap. The first method used was extending root cutouts while increasing the chord on the remainder of the blade to maintain the high thrust-weighted solidity. The second method was to reduce the amount of blade taper such that overall chord scaling was reduced due to more blade area closer to the blade tip.

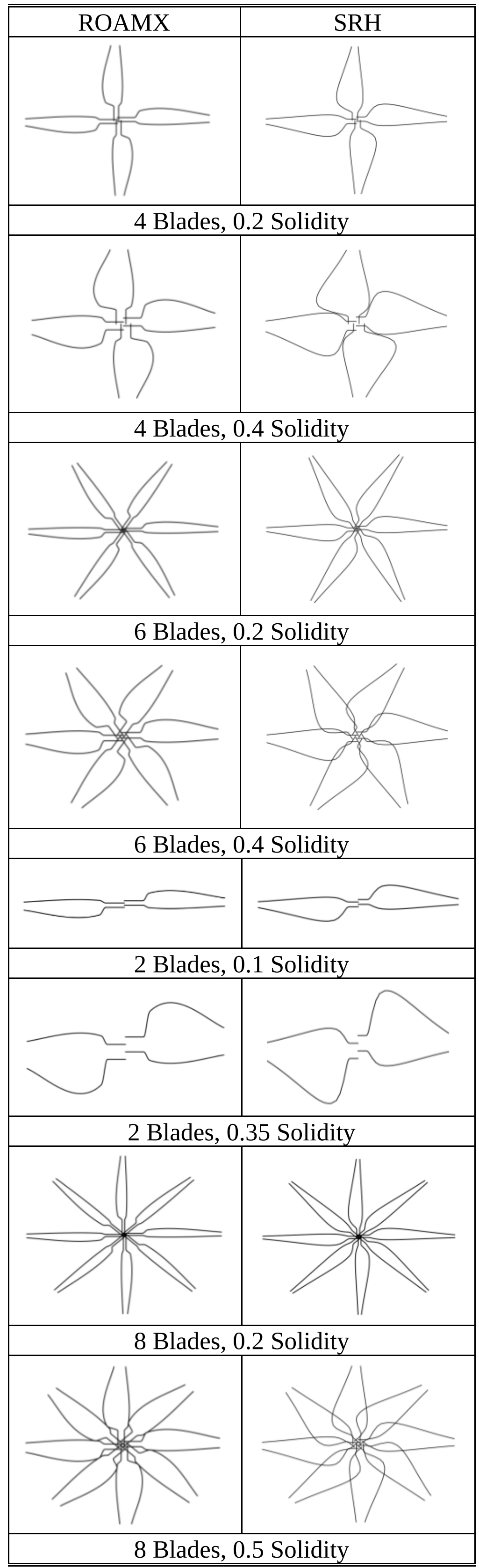

Figure 3. Various ROAMX and SRH Rotor Configurations.

Reynolds Number Correction

Considerations were needed for the change in Reynolds number, as fewer blades at the same solidity necessarily have larger chords. Since the airfoil tables used for both rotors were specifically for blades with the original blade chord, Reynolds number effects needed to be considered as larger Reynolds numbers are experienced by the larger blades. To quantify this effect, another set of airfoil tables was generated for the SRH rotor at a lower density and consequently lower Reynolds number. The density used to generate the original airfoil tables for SRH was 0.0156 kg/m^3 and the new airfoil tables for SRH were generated with a density of 0.0123 kg/m^3. The same CAMRAD II analyses were run with the new airfoil tables to observe the effect of Reynolds number on performance (as an example of prior research in this area see [Refs. 13 and 14]). Scaling the rotor profile power or the airfoil drag with a function of Reynolds number is a common approach for correcting small-scale wind tunnel performance results to full scale [Ref. 14]. At large Reynolds numbers, it is appropriate to scale the rotor drag with Re^n, with $n = 0.2$; for the very small Reynolds numbers of operation on Mars, a large scaling exponent is expected. Profile power outputs of the higher density results were scaled such that the figure of merit calculated with the scaled profile power resulted in figure of merit values resembling the lower density results. The profile power scale factor that worked for SRH at all blade numbers was 1.1. With the Reynolds number ratio of 0.7884 (just due to the density ratio for these calculations), the scaling exponent is $n = 0.4$. This approach was also utilized for the ROAMX rotor with additional 0.01 kg/m^3 and 0.02 kg/m^3 density airfoil tables. A Reynolds number scaling exponent of 0.4 was found to be appropriate for ROAMX as well. Note that scaling profile power is equivalent to scaling all drag values in the airfoil tables by the same factor. Then to correct the performance calculations using fixed airfoil tables, with varying chord at the same atmosphere and tip speed, the chord ratio gives the Reynolds number ratio for profile power scaling.

As observed in Figures 4 and 5, applying the Reynolds number correction reveals higher performance of both SRH and ROAMX blades than the uncorrected results, with a slightly larger effect on the SRH rotor. The Reynolds number scaling has the largest effect for smaller blade numbers. All following performance calculations presented include the Reynolds corrections.

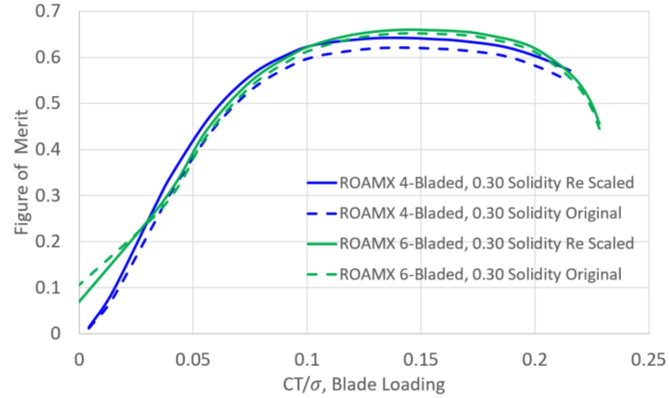

Figure 4. Reynolds number correction effect for ROAMX.

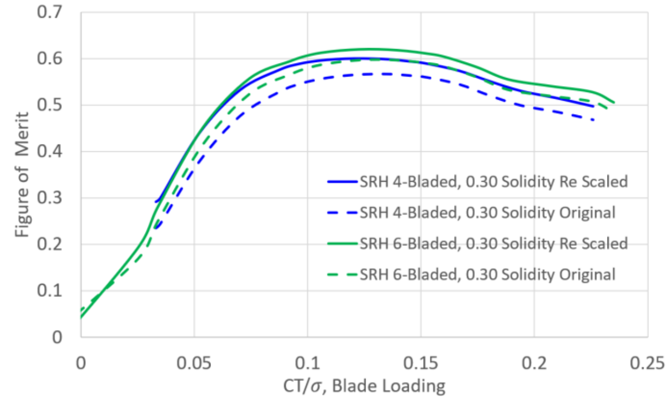

Figure 5. Reynolds number correction effect for SRH.

EFFECTS OF SOLIDITY AND NUMBER OF BLADES

Solidity Effects

As observed in Figures 6-13, for both rotors, peak figure of merit is achieved between the blade loading range of 0.1 and 0.2. As solidity increases, the blade loading required to achieve the peak figure of merit decreases. A significant decrease in figure of merit is observed at solidities below 0.2 for blade numbers higher than two and above 0.3 for numbers lower than eight. Convergence issues were encountered for the ROAMX rotor for the 2-bladed configuration above a solidity of 0.2, for the 4-bladed configuration at high blade loading for solidities above 0.3, and for the 8-bladed configuration at high blade loading for solidities below 0.4.

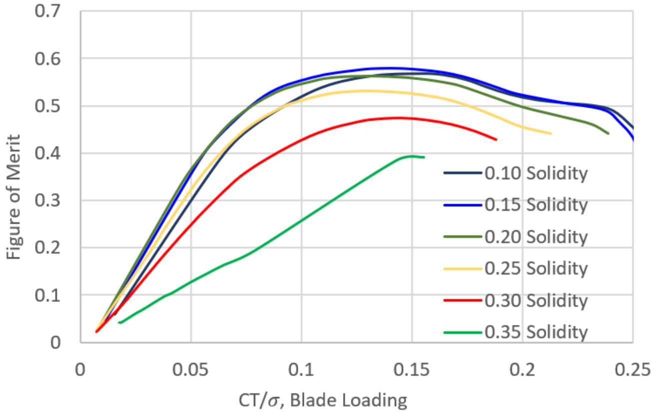

Figure 6. Effect of solidity on figure of merit for 2-bladed SRH configuration.

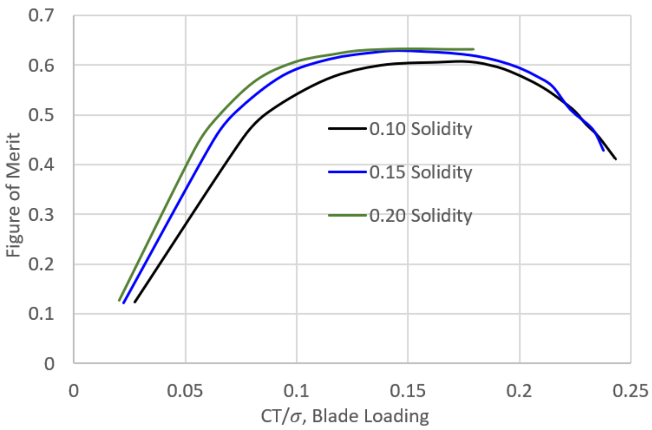

Figure 7. Effect of solidity on figure of merit for 2-bladed ROAMX configuration.

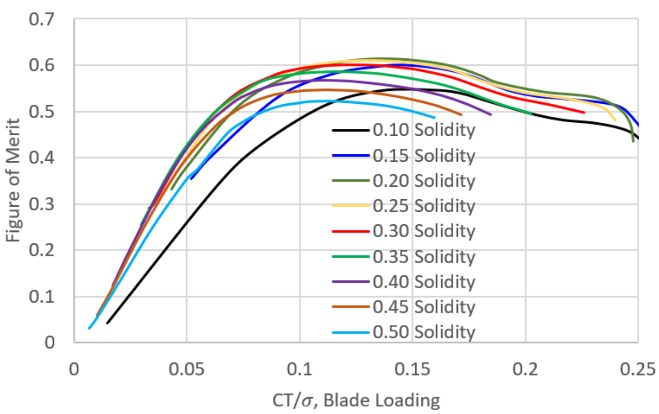

Figure 8. Effect of solidity on figure of merit for 4-bladed SRH configuration.

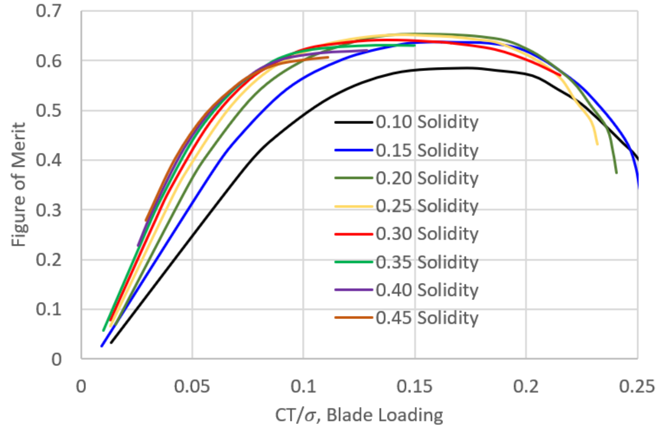

Figure 9. Effect of solidity on figure of merit for 4-bladed ROAMX configuration.

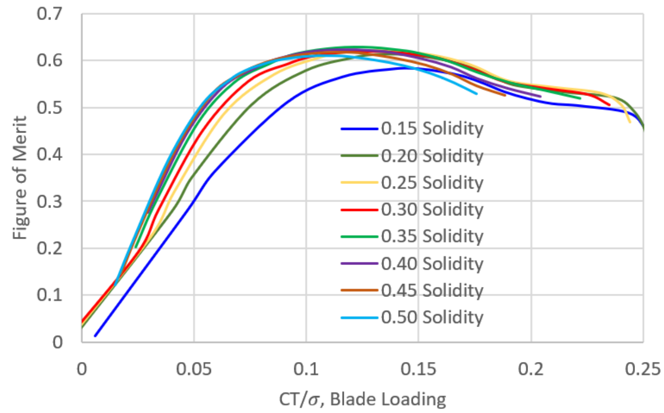

Figure 10. Effect of solidity on figure of merit for 6-bladed SRH configuration.

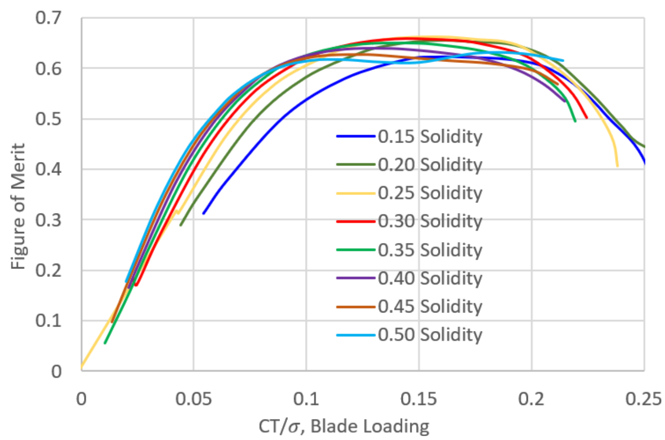

Figure 11. Effect of solidity on figure of merit for 6-bladed ROAMX configuration.

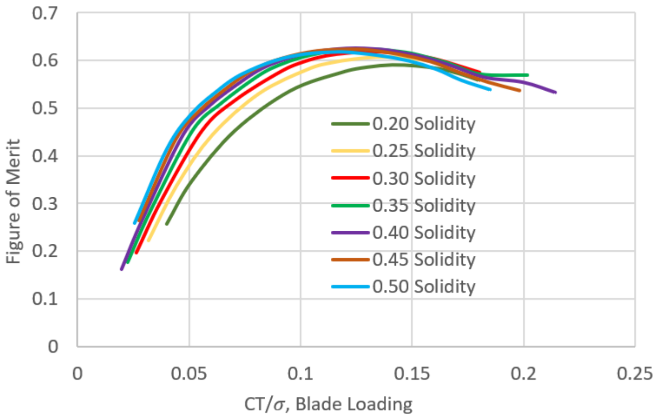

Figure 12. Effect of solidity on figure of merit for 8-bladed SRH configuration.

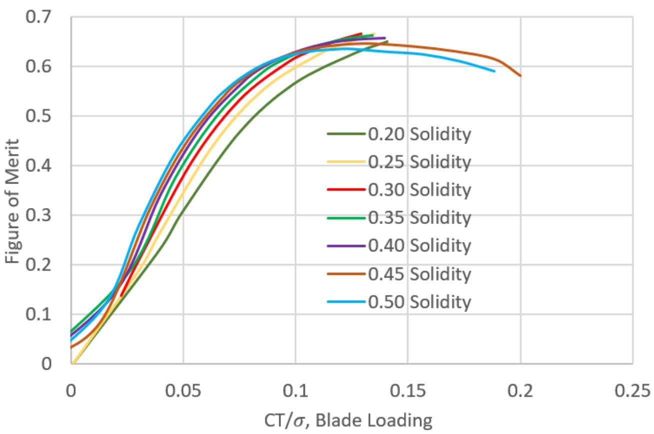

Figure 13. Effect of solidity on figure of merit for 8-bladed ROAMX configuration.

Number of Blades Effects

As seen in Figures 14 and 15, increasing blade number increases figure of merit at high blade loading and decreases figure of merit at low blade loading. Increasing blade count from 4 to 6 increases figure of merit at a blade loading of 0.15 by 3.6% for SRH and 2.9% for ROAMX. There is a penalty of 7.3% and 1.8%, respectively, in figure of merit for the SRH and ROAMX 8-bladed configurations as compared to their 6-bladed configurations for a blade loading of 0.08. However, the difference between six and eight blades for SRH at high blade loading is minimal, and the 8-bladed configuration with solidity values below 0.45 had convergence issues above a blade loading of 0.15. Also, accounting for increased hub complexity and blade overlap of higher blade numbers it is clear that a 6-bladed configuration is ideal with respect to figure of merit. As observed in Figure 14, figure of merit is significantly lower for the SRH 2-bladed configuration. The 2-bladed ROAMX configurations above 0.2 solidity did not converge.

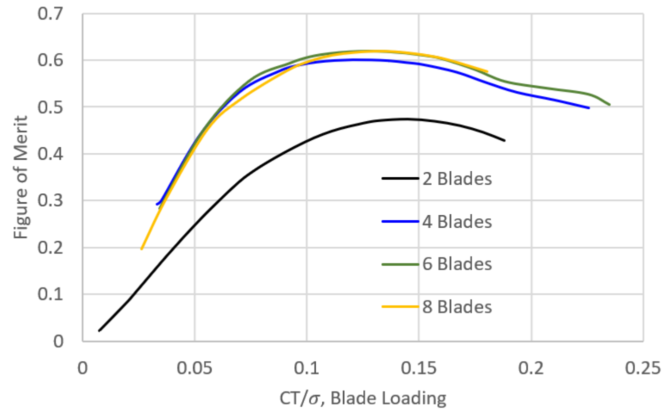

Figure 14. Effect of number of blades on figure of merit for 0.3 solidity SRH configuration.

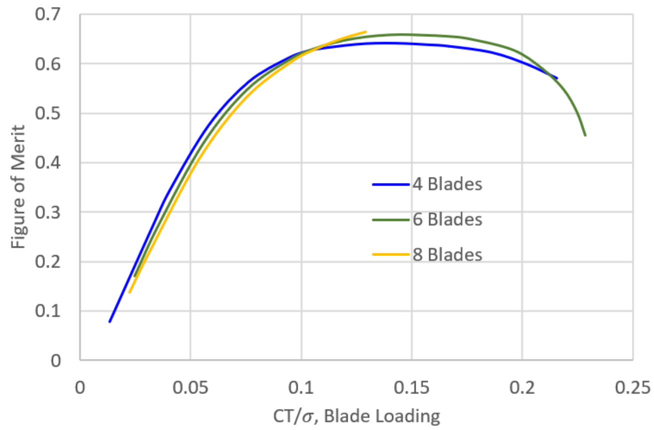

Figure 15. Effect of number of blades on figure of merit for 0.3 solidity ROAMX configuration.

As observed in Figures 6-15, the ideal configuration with respect to figure of merit is the 6-bladed 0.3 solidity configuration for both rotors. Figure 16 shows the effect of both blade number and solidity on peak figure of merit of the ROAMX rotor. While increasing number of blades improves performance, it also increases mechanical complexity. Additionally, as observed in Figure 17, increasing solidity increases thrust. For these reasons, the ideal case examined in this study is the 6-bladed configuration with a solidity of 0.30 for both rotors, with the ROAMX rotor outperforming the SRH rotor.

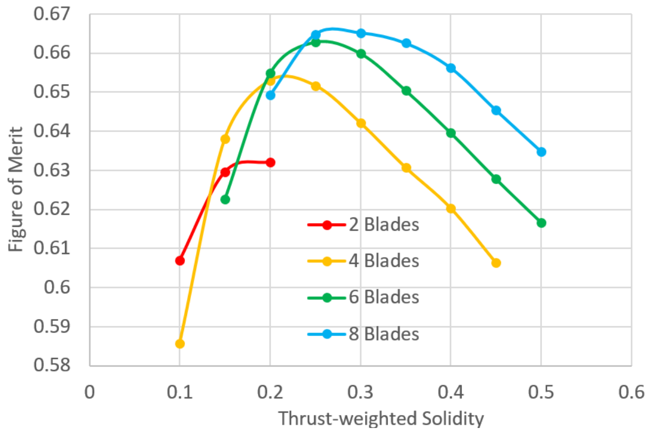

Figure 16. Peak figure of merit vs thrust-weighted solidity for ROAMX airfoils with varying number of blades

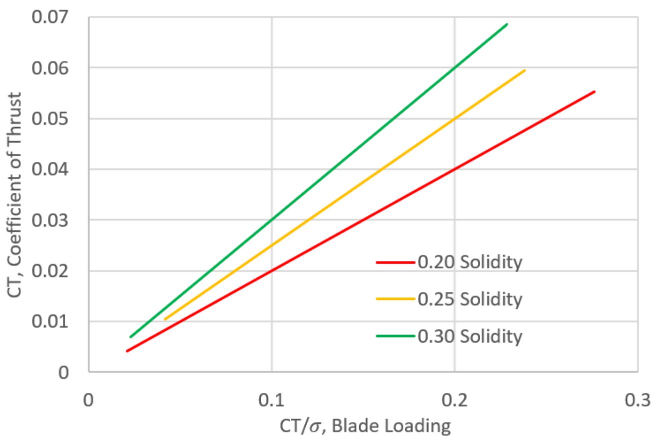

Figure 17. Coefficient of thrust vs blade loading for ROAMX 6-bladed configuration with varying solidity

ROOT CUTOUT AND TAPER RATIO MODIFICATION EFFECTS

As a preliminary approach to determine if there were practical modifications to be made to the blades while maintaining solidity, varying root cutouts and taper modifications were used to avoid blade overlap in the scaled rotor blades. A scaled blade, prior to modification, has a root cutout of 10% and a taper ratio of -0.22. The results provided in Figures 18 and 19 show that root cutouts greater than 20% of the rotor radius result in significantly degraded performance and less tapered blades result in a decrease in performance, but to a much lesser degree than root cutout. While both methods can alleviate blade overlap concern, for very high rotor solidities, more blade overlap requires drastic changes in blade shape, which necessitates completely redesigned blades. Therefore, it is necessary to avoid scaling to a blade design that introduces overlap.

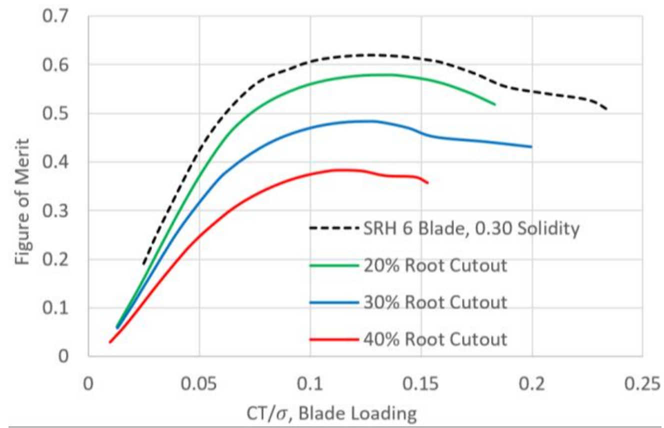

Figure 18. Root cutout effects for SRH 6-bladed 0.3 solidity rotor

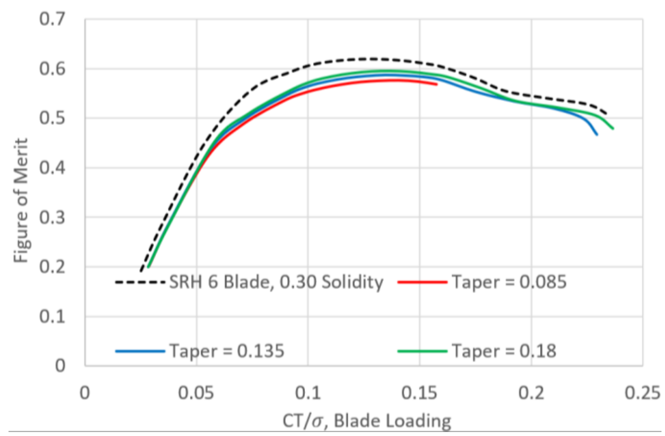

Figure 19. Taper effects for SRH 6-bladed 0.3 solidity rotor

CONCLUSIONS

1. Reynolds number scaling increases performance of high solidity rotors with airfoil tables for lower solidity (lower Reynolds number) blades. The largest effect is observed for configurations with fewer blades. For more accurate performance calculations, airfoil tables for specific geometry and atmosphere are needed.
2. Figure of merit increases with increasing solidity up to roughly 0.3. Beyond 0.3 solidity, figure of merit decreases. Increasing solidity also reduces the blade loading required for peak figure of merit.
3. Increasing the number of blades increases figure of merit. However, increasing the number of blades beyond six only marginally increases figure of merit.
4. Increasing root cutout to avoid blade overlap significantly decreases figure of merit.
5. Reducing taper ratio to avoid blade overlap at the root slightly decreases figure of merit.
6. Root cutout and taper ratio modifications are not sufficient for blade overlap remediation of the high solidity high blade number configurations. As such,

a complete blade redesign is necessary for these configurations.

7. For both the SRH and ROAMX rotors, the ideal configuration with respect to figure of merit is the 6-bladed with 0.3 solidity. The ROAMX rotor outperforms the SRH rotor in all configurations.

Author contact:
Gianmarco Sahragard-Monfared G.Monfared@nasa.gov

ACKNOWLEDGMENTS

The authors thank Dr. Dorcas Kaweesa, Ethan Romander, and Sesi Kottapalli for reviewing this document and providing valuable feedback. The authors acknowledge the Mars Exploration Program (MEP) and the Convergent Aeronautics Solutions (CAS) Project for funding and support of this work.

REFERENCES

[1] Balaram, J., Canham, T., Duncan, C., Golombek, M., Grip, H.F., Johnson, W., Maki, J., Quon, A., Stern, R., and Zhu, D., "Mars Helicopter Technology Demonstrator," AIAA Atmospheric Flight Mechanics Conference, AIAA SciTech Forum, Kissimmee, FL, 2018.

[2] Koning, W., Perez Perez, N., Cummings, H.., Romander, E.A., and Johnson, W., "ELISA: A Tool for Optimization of Rotor Hover Performance at Low Reynolds Number in the Mars Atmosphere," Journal of the American Helicopter Society, Volume 69, Number 4, October 2024, pp. 1-15(15).

[3] Cummings, H., Perez Perez, N., Koning, W., Johnson, W., Young, L., Haddad, F., Romander, E., Balaram, J., Tzanetos, T., Bowman, J., Wagner, L., Withrow-Maser, S., Isaacs, E., Toney, S., Shirazi, D., Conley, S., Pipenberg, B., Datta, A., Lumba, R., Chi, C., Smith, K., Cornelison, C., Perez, A., Nonomura, T., and Asai, K., "Overview and Introduction of the Rotor Optimization for the Advancement of Mars eXploration (ROAMX) Project," 2022 Transformative Vertical Flight Conference, San Jose, CA, January 2022.

[4] Koning, W.J.F., Perez Perez, N., Cummings, H., Nagata, T., Kanzaki, Y., Kasai, M., Miyagi, M., Nonomura, T., Asai, K., Caros, L., Buxton, O., Vincent, P., "Experimental Results for Mars Rotorcraft Airfoils (roamx-0201 and clf5605) at Low Reynolds Number and Compressible Flow in a Mars Wind Tunnel," NASA/TM-20240004230, Moffett Field, California, April 2024.

[5] Johnson, W., Withrow-Maser, S., Young, L., Malpica, C., Koning, W.J.F., Kuang, W., Fehler, M., Tuano, A., and Chan, A., "Mars Science Helicopter Conceptual Design," NASA/TM- 2020–220485, Moffett Field, California, March 2020.

[6] Koning, W.J.F., Johnson, W., and Grip, H.F., "Improved Mars Helicopter Aerodynamic Rotor Model for Comprehensive Analyses," AIAA Journal, Volume 57, Number 9, July 2019, pp. 3969-3979.

[7] Koning, W., Allan, B.G., Romander, E.A., and Johnson, W., "Comparing 3D and 2D CFD for Mars Helicopter Ingenuity Rotor Performance Prediction," 49th European Rotorcraft Forum, Buckeburg, German, September 2023

[8] Schatzman, N., Chan, A., Fillman, M., Meyn, L., Gehlot, V., Glazebrook, K., Santillian, D., and Ridland, P., "Performance Analysis and Data Processing for the Mars Sample Recovery Helicopter in the Jet Propulsion Laboratory 25-ft Space Simulator," Vertical Flight Society's 80th Annual Forum and Technology Display, Montreal, Quebec, May 2024.

[9] Schatzman, N., Chan, A., Gehlot, V., and Glazebrook, K., "Data Processing and Analysis of Performance Measurements from Ingenuity Rotors in the Jet Propulsion Laboratory 25-Ft Space Simulator," 2024 Transformative Vertical Flight Conference, Santa Clara, CA, February 2024.

[10] Withrow-Maser, S., Johnson, W., Tzanetos, T., Grip, H., Koning, W., Schatzman, N., Young, L., Chan, A., Ruan, A., Cummings, H., Allan, B., Malpica, C., Meyn. L., Pipenberg, B., and Keenon, M., "Mars Sample Recovery Helicopter: Rotorcraft to Retrieve the First Samples from the Martian Surface," Vertical Flight Society's 79th Annual Forum and Technology Display, West Palm Beach, FL, May 2023.

[11] Wright, S., Sahragard-Monfared, G., Schatzman, N.L., Johnson, W., Ridland, P., and Fillman, M., "Comprehensive Analysis Aeroelastic Stability Predictions for the Mars Sample Recovery Helicopters and Ingenuity," 2024 Transformative Vertical Flight Conference, Santa Clara, CA, February 2024.

[12] Ågren, T., Peters, N., Ruan, A., "Rotor Wake Modeling for Mars Rotorcraft using the Viscous Vortex Particle Method," Vertical Flight Society's 81st Annual Forum and Technology Display, Virginia Beach, VA, May 2025.

[13] Yamauchi, G.K., and Johnson, W., "Trends of Reynolds Number Effects on Two-Dimensional Airfoil Characteristics for Helicopter Rotor Analyses," NASA/TM- 84363, Moffett Field, California, April 1983.

[14] Keys, C.N., McVeigh, M.A., Dadone, L., and McHugh, F.J., "Estimation of Full-Scale Rotor Performance from Model Rotor Test Data," Journal of the American Helicopter Society, Volume 30, Number 4, October 1985.